Biochimica et Biophysica Acta, 778 (1984) 470–480
Elsevier

BBA 72365

CHARACTERIZATION OF THE SIZE DISTRIBUTION OF UNILAMELLAR VESICLES BY GEL FILTRATION, QUASI-ELASTIC LIGHT SCATTERING AND ELECTRON MICROSCOPY

P. SCHURTENBERGER [a] and H. HAUSER [b]

[a] *Laboratorium für Festkörperphysik, ETH-Hönggerberg, CH-8093 Zürich and* [b] *Laboratorium für Biochemie, Eidgenössische Technische Hochschule, CH-8092 Zürich (Switzerland)*

(Received June 18th, 1984)

Key words: Phospholipid vesicle; Size distribution; Gel filtration; Quasi-elastic light scattering; Electron microscopy

The size and size distribution of unilamellar phospholipid vesicles present in unsonicated phosphatidic acid and mixed phosphatidic acid/phosphatidylcholine dispersions were determined by gel filtration, quasi-elastic light scattering and freeze-fracture electron microscopy. The vesiculation in these dispersions was induced by a transient increase in pH as described previously (Hauser, H. and Gains, N. (1982) Proc. Natl. Acad. Sci. USA 79, 1683–1687). The resulting phospholipid dispersions are heterogeneous consisting of small unilamellar vesicles (average radius $r < 50$ nm) and large unilamellar vesicles (average r ranging from about 50 to 500 nm). The smallest vesicles with $r = 11 \pm 2$ nm are observed with dispersions of pure phosphatidic acid, the population of these vesicles amounting to about 80% of the total lipid. With increasing phosphatidylcholine content the radius of the small unilamellar vesicles increases and at the same time the population of small unilamellar vesicles decreases. The average radius of small unilamellar vesicles present in phosphatidic acid/phosphatidylcholine dispersions (mole ratio, 1:1) is 17.5 ± 2 nm, the population of these vesicles amounting to about 70% of the total lipid. By a combination of gel filtration, quasi-elastic light scattering and freeze-fracture electron microscopy it was possible to characterize the large unilamellar vesicles. This population is heterogeneous with its mean radius also increasing with increasing phosphatidylcholine content. After separating the large unilamellar vesicles from small unilamellar vesicles on Sepharose 4B it can be shown by quasi-elastic light scattering that in pure phosphatidic acid dispersions 80–90% of the large unilamellar vesicle population consist of vesicles with a mean radius of 170 nm. In mixed phosphatidic acid/phosphatidylcholine dispersions this radius increases to about 265 nm as the phosphatidylcholine content is raised to 90 mol%.

Introduction

Liposomes, in the form of both multilamellar structures and unilamellar vesicles, are of interest as models for biological membranes and as potential drug delivery systems. The aim of the latter application is to direct the encapsulated drug to specific sites in the body and this potential use of liposomes has stimulated the development of new methods for the preparation of unilamellar vesicles [1,2]. Recently, we described a simple and quick method for the preparation of unilamellar vesicles of phosphatidic acid (PA) and mixtures of phosphatidylcholine (PC) and PA [3]. The method essentially consists of a transient increase in pH so that the phosphate group of PA becomes fully ionized. It avoids tedious procedures such as soni-

Abbreviations: PC, egg phosphatidylcholine; PA, egg phosphatidic acid.

cation or detergent removal by dialysis or gel filtration. The resulting phospholipid dispersion was shown to comprise small unilamellar vesicles of a relatively narrow particle size distribution and large unilamellar vesicles [3–5] of a wide size distribution. More recently we showed that this method of forming unilamellar vesicles by pH adjustment is not restricted to PA and mixed PC/PA dispersions, but that the principle underlying this method is a general one. It is applicable to any lipid mixture containing PA that forms a smectic lamellar phase in H_2O [5,6]. Furthermore, it is possible to replace PA by amphiphiles carrying an ionizable group [6].

In order to assess the usefulness of this method and its possible applications it is important to characterize the resulting vesicle preparation in terms of their particle size distribution and to show how this size distribution changes as a function of experimental conditions, e.g., the PA content. Here we characterize in terms of size and size distribution unsonicated dispersions of pure PA and different PA/PC mixtures prepared by the method of pH change. Particle size inhomogeneity has so far precluded a detailed characterization of such dispersions, particularly of the population of large vesicles with a diameter greater than 100 nm [3–6]. A satisfactory solution to the problem was obtained by using a combination of different techniques: gel filtration on Sepharose 4B and Sephacryl S 1000, quasi-elastic light scattering and electron microscopy. The merits of the different methods used here will be discussed.

Materials and Methods

Egg phosphatidic acid and egg phosphatidylcholine were purchased from Lipid Products (South-Nutfield, U.K.). The phospholipids were pure by TLC standards. Sepharose 4B and Sephacryl S 1000 were obtained from Pharmacia Fine Chemicals AB (Zürich, Switzerland), and Dow Latex beads of different sizes from Serva Feinbiochemica (Heidelberg, F.R.G.). The Sepharose 4B column was calibrated using the following marker proteins: horse myoglobin, rabbit muscle aldolase, horse liver catalase, ferritin from horse spleen and thyroglobulin from hog thyroid gland (all from Serva Feinbiochemica, Heidelberg, F.R.G.). Brome mosaic virus, also used as a calibration standard, was a gift from Dr. M. Zulauf.

Unsonicated phospholipid dispersions were prepared and the vesiculation induced by a transient pH change as described before [3–5]. Gel filtration on Sepharose 4B was carried out essentially as described previously [4,7]. Before applying the dispersions to the Sepharose 4B column they were centrifuged in 1.5-ml tubes for 3 min at $12000 \times g$ to remove very large liposomes that could clog the column. This centrifugation procedure usually pelleted not more than 5–10% of the total phospholipid except for PC-rich dispersions (PA/PC, mole ratio 1 : 9) where the loss was 10–20%. In order to obtain reproducible elution profiles the column was presaturated with the appropriate phospholipid dispersion. With presaturated columns recoveries were $92 \pm 9\%$ ($n = 13$). The Sepharose 4B column was calibrated using different marker proteins and brome mosaic virus. The Stokes radii of the marker proteins were calculated from their diffusion coefficients D * taken from the literature. The calibration data were evaluated according to the procedure of Ackers [8] relating the hydrodynamic radius r to the column parameter K_d:

$$r = a_o + b_o \, \mathrm{erf}^{-1}(1 - K_d) \qquad (1)$$

where a_o and b_o are constants characteristic of the gel filtration medium and $K_d = (V_e - V_o)/(V_t - V_o)$, V_e = elution volume and V_o and V_t are the void volume and total column volume, respectively. The calibration curve thus obtained is shown in Fig. 1A. Phospholipid dispersions were also chromatographed on Sephacryl S 1000 which was handled similarly to Sepharose 4B. The calibration (see Fig. 1B) was carried out with Latex beads of

* The attempt to determine D by quasi-elastic light scattering failed. For this purpose the proteins dissolved in the proper buffer solution were dialyzed exhaustively against the same buffer and before measurement the solutions were centrifuged at $100000 \times g$ for 30 min. The hydrodynamic radii thus obtained were significantly larger than the Stokes radii calculated from the classical diffusion constant D. This is probably due to quasi-elastic light scattering being particularly sensitive to the presence of protein oligomers. That protein aggregates were indeed present was evident from the high polydispersity index (50–60%) of these solutions.

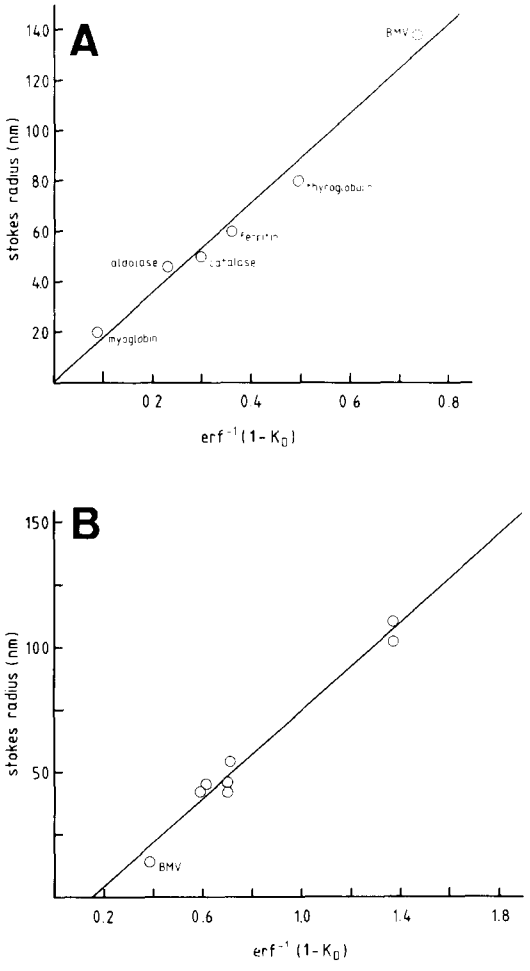

Fig. 1. Calibration of (A) Sepharose 4B and (B) Sephacryl S 1000. Sepharose 4B (45×0.9 cm) was equilibrated with 0.15 M NaCl/0.01 M Hepes (pH 7.5)/0.02% NaN_3. The void volume $V_o = 12$ ml (fraction No. 40) was determined using Dextran blue, Latex beads of diameter 109 nm, or large phospholipid liposomes, and the total column volume $V_t = 33$ ml (fraction No. 111) was obtained by chromatographing radioactive D-glucose, inorganic phosphate, or dinitrophenyl-L-alanine solutions. Sephacryl S 1000 (34×1 cm) was equilibrated with 0.01 M Hepes (pH 7.4)/0.3 M mannitol/5 mM EDTA/0.02% NaN_2/0.01 M sodium dodecyl sulfate. The void volume $V_o = 13.2$ ml (fraction No. 23) was determined by chromatographing in SDS buffer Latex beads of diameter = 481 nm. The total column volume $V_t = 33.6$ ml (fraction No. 59) was determined with myoglobin, dinitrophenyl-L-alanine and $CuSO_4$ which all gave consistent results within the error of the measurement. Brome mosaic virus was used as a calibration standard for both Sepharose 4B and Sephacryl S 1000. In this case, the column was equilibrated and eluted with 0.1 M potassium acetate (pH 4.8) containing 5 mM $MgCl_2$. BMV, brome mosaic virus.

known diameter: 220 ± 6.5, 109 ± 2.7, 91 ± 5.8 and 85 ± 5.5 nm and with brome mosaic virus. The Latex beads were dispersed in buffer containing 10 mM SDS in order to prevent their aggregation and the Sephacryl column was also run with this buffer [9].

The light scattering apparatus consists of an argon ion laser (Spectra Physics, model 171, λ = 514.5 nm), a temperature-controlled scattering cell holder, a digital autocorrelator (Malvern K 7023, 96 channels) and an on-line data analysis performed on a Nova 3 computer (for details, see Ref. 10).

Sample purification and data analysis have been described in detail [11]. The mean diffusion coefficient $\bar{D}$ and the polydispersity V (as defined in Ref. 12) were determined by means of a cumulant analysis of the intensity autocorrelation function [13]. From $\bar{D}$ an apparent mean hydrodynamic radius $\bar{r}_h$ as defined by Eqn. 2 was calculated [11].

$$\bar{r}_h = \frac{kT}{6\pi\eta\bar{D}} \tag{2}$$

where η is the viscosity of the solvent, k is Boltzmann's constant and T is the absolute temperature. The normalized intensity autocorrelation function $c(\tau)$ was also analyzed in terms of two discrete particle sizes with diffusion coefficients D_1 and D_2 and relative intensities G_1 and $1 - G_1$, respectively [14].

$$c(\tau) = B + \left(G_1 \cdot \exp\left(-D_1 \cdot q^2 \cdot \tau\right) + (1 - G_1)\exp\left(-D_2 \cdot q^2 \cdot \tau\right)\right)^2 \tag{3}$$

where q is the scattering vector. For some samples a third approach was used: the correlation functions measured at various sampling times were mathematically spliced together to give a normalized correlation function $c'(\tau)$ extended over a large range of τ [15]. $c'(\tau)$ was analyzed using Eqn. 4

$$c'(\tau)^{1/2} = G_1 \exp\left(-D_1 q^2 \tau\right) + G_2 \exp\left(-D_2 q^2 \tau\right) + (1 - G_2 - G_3)\exp\left(-D_3 q^2 \tau\right) \tag{4}$$

Eqn. 4 represents the square root of a normal-

ized intensity autocorrelation function of a sample consisting of three discrete components with diffusion coefficients D_1, D_2, D_3 and relative intensities G_1, G_2 and $(1 - G_1 - G_2)$, respectively. The computer program used allowed any of the five parameters (D_1, D_2, D_3, G_1, G_2) to be treated as either fixed or variable. The apparent hydrodynamic radius of the individual components, r_i, was calculated from the D_i value using Eqn. 2.

Samples for electron microscopy were prepared as described previously [5].

Results

Gel filtration

Unless otherwise stated, unsonicated dispersions of PA and various mixtures of PA and PC were prepared in H_2O as described previously [3–5]. They were then applied to a Sepharose 4B column equilibrated with 10 mM Hepes pH 7.5/0.15 M NaCl/0.02% NaN_3. The elution profile of the PA dispersion is shown in Fig. 2A, the elution profiles of two mixed PA/PC dispersions are shown in Fig. 3A (PA/PC, mole ratio 1 : 1) and Fig. 4A (PA/PC, mole ratio 1 : 9). PA dispersions gave reproducibly an elution profile consisting of two peaks, the first one (peak I) eluting at the void volume of the column and comprising about 22% of the total phospholipid applied, the second peak (II) eluting at fraction number 72 ($K_d = 0.49$ column volumes) and comprising 78% of the applied lipid. The Stokes radius determined from the elution volume V_e of peak II was 9.4 nm. Similar elution profiles as shown in Fig. 2A were obtained with mixed PA/PC dispersions containing an excess of PA (data not shown). As the PC content increased, the elution volume and the area of peak II decreased. At the same time the area of peak I grew apparently at the expense of peak II. This is demonstrated in Fig. 3A showing as an

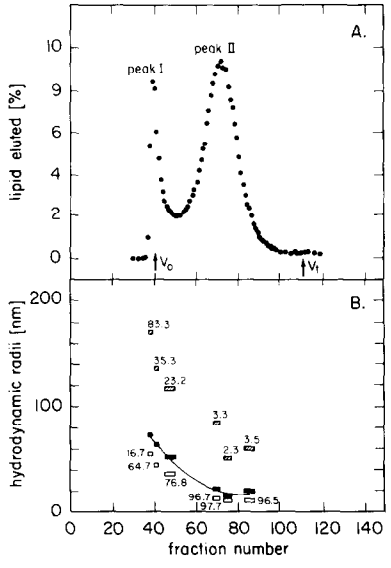

Fig. 2. (A) Elution profile from Sepharose 4B of an unsonicated PA dispersion (0.8 ml of approx. 1%) prepared in H_2O as described previously [3–5]. The lipid was applied to the column and eluted with the column buffer (0.3 ml fractions, flow rate 2.5–3 ml/h). Phospholipid concentrations were determined by phosphate analysis [18]. (B) Hydrodynamic radii determined by quasi-elastic light scattering of vesicles present in various fractions of the elution profile shown in (A). Given are the mean hydrodynamic radius $\bar{r}_h$ calculated from a cumulant analysis (■) and the hydrodynamic radii of the small (□) and large component (▨) together with the weight fractions (%) obtained from a two-component analysis (see text). The length of the horizontal bars indicates the number of fractions of the above elution profile (A) that were pooled and analyzed by quasi-elastic light scattering.

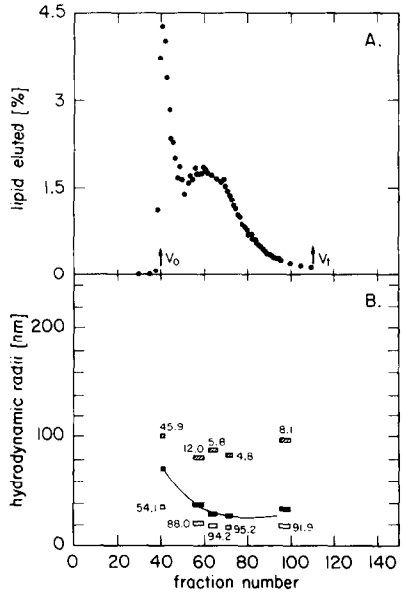

Fig. 3. (A) Elution profile from Sepharose 4B of an unsonicated mixed dispersion of PA/PC (mole ratio, 1:1) prepared in water (0.8 ml of approx. 1%). (B) Hydrodynamic radii determined by quasi-elastic light scattering of vesicles present in various fractions of the elution profile shown in (A). For details see legend of Fig. 2B.

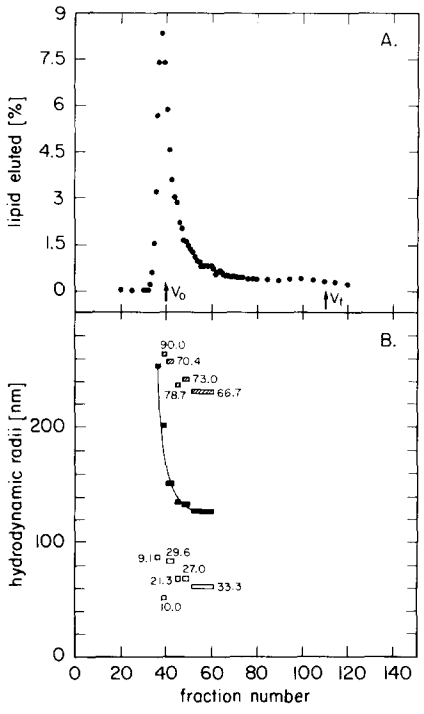

Fig. 4. (A) Elution profile from Sepharose 4B of an unsonicated mixed dispersion of PA/PC (mole ratio, 1:9) prepared in water (0.8 ml of approx. 1%). (B) Hydrodynamic radii determined by quasi-elastic light scattering of vesicles present in various fractions of the elution profile shown in (A). For details, see legend of Fig. 2B.

example a PA/PC dispersion (mole ratio, 1:1). The two peaks are less well resolved than those of the pure PA dispersion in Fig. 2A. From the elution volume of peak II (fraction No. 60; K_d = 0.23–0.29 column volumes) a mean Stokes radius of 13.5–15.2 nm was estimated using the calibration curve in Fig. 1A.

On further increasing the PC content the elution volume of peak II decreased and eventually peaks I and II merged. For instance, PA/PC dispersions with mole ratios smaller than 3:7 eluted as a single asymmetric peak at the void volume, indicating that most of the lipid is present as large particles that are excluded from the column matrix (Fig. 4A).

The same PA/PC dispersion (mole ratio, 1:1) as chromatographed in Fig. 3A was applied to a Sephacryl S 1000 column. A typical elution profile is shown in Fig. 5A. Similar to the gel filtration on Sepharose 4B, the particles of such a dispersion were separated reproducibly into two, partly resolved peaks. The first peak (I) eluted near the void volume of the column (fraction No. 30; K_d = 0.2 column volumes) and the second one at fraction No. 44 (K_d = 0.58 column volumes), corresponding to mean Stokes radii of 67 and 20 nm, respectively. The column chromatogram of a PC/PA lipid dispersion (mole ratio, 1:1), which was

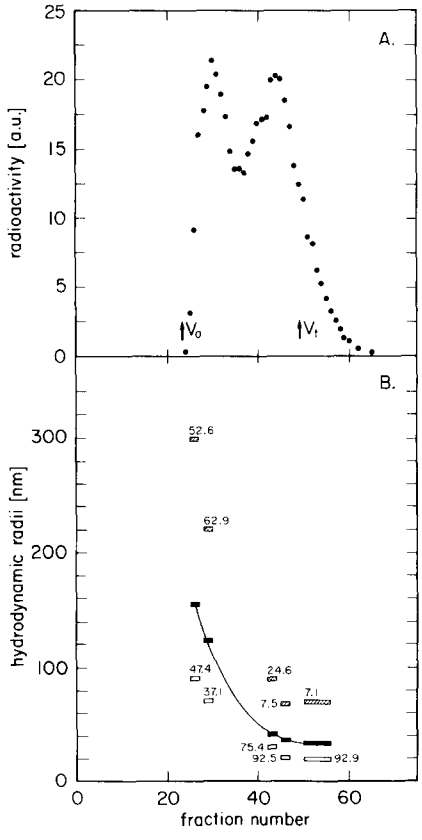

Fig. 5. (A) Elution profile from Sephacryl S 1000 of an unsonicated mixed dispersion of PA/PC (mole ratio, 1:1) prepared in water; 0.6 ml of approx. 1% dispersion were applied and eluted with the column buffer (0.01 M Hepes (pH 7.4)/0.3 M mannitol/5 mM EDTA/0.02% NaN_3; 0.57 ml fractions, flow rate 6–7 ml/h). The phospholipid concentrations in the eluate were determined by P-analysis [18] or by liquid scintillation counting. In the latter case trace amounts of [^{3}H]dipalmitoylphosphatidylcholine were mixed with the lipids. The recovery of phospholipid in the eluate was approx. 90%. (B) Hydrodynamic radii determined by quasi-elastic light scattering of vesicles present in various fractions of the elution profile shown in (A). For details see legend of Fig. 2B.

TABLE I

QUASI-ELASTIC LIGHT SCATTERING AND ELECTRON MICROSCOPY RESULTS OBTAINED WITH UNSONICATED PA AND PA/PC DISPERSIONS

$\bar{r}$ is the weighed average radius derived from freeze-fracture electron microscopy (EM). For details see text. For the quasi-elastic light scattering analysis (QLS), r_1 and r_2 were derived from a two-component analysis using Eqn. 3 and the weight fractions W_1 and W_2 were determined using Eqn. 6. For the gel filtration results, W_1 and W_2 are the percentages of phospholipid eluted in peak I and II of the Sepharose 4B chromatogram, respectively. The mole ratio of PA/PC is presented in parentheses.

Sample	QLS $\bar{r}_h$ (nm)	EM $\bar{r}$ (nm)	Quasi-elastic light scattering, two-component analysis				Gel filtration on Sepharose 4B	
			r_1 (nm)	W_1 (%)	r_2 (nm)	W_2 (%)	W_1 (%)	W_2 (%)
PA	42.0	50.8	86	18	20.5	82	22	78
PA/PC (1:1)	45.0	62.0	77	24	24	76	28	71
PA/PC (1:9)	140.0	148.0	364	80	66	20	–	–

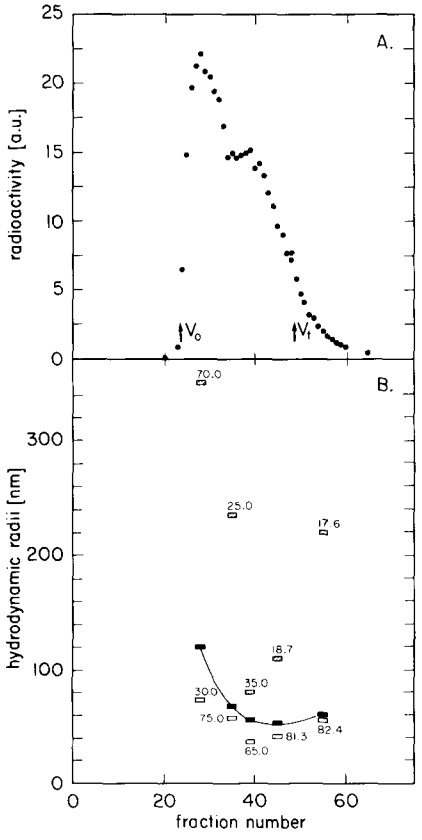

Fig. 6. (A) Elution profile from Sephacryl S 1000 of an unsonicated mixed dispersion PA/PC (mole ratio, 1:1) prepared in column buffer (0.6 ml of approx. 1%). (B) Hydrodynamic radii determined by quasi-elastic light scattering of vesicles present in various fractions of the elution profile shown in (A). For details see the legend of Fig. 2B.

dispersed in column buffer instead of water, is shown for comparison in Fig. 6A. Under these conditions peak I and II were less well resolved; peak II eluted earlier (at fraction 38; $K_d = 0.44$ column volumes) indicating that it consists of larger particles than the second peak of Fig. 5A. The mean Stokes radii of peak I and II derived from the elution volumes were 73 and 35 nm, respectively.

Quasi-elastic light scattering

The same dispersions which were subjected to gel filtration (Figs. 2–5) were analyzed by quasi-elastic light scattering. The results are summarized in Table I.

The mean hydrodynamic radius $\bar{r}_h$ derived from a cumulant analysis of the intensity autocorrelation function increased with increasing PC content. $\bar{r}_h$ derived from quasi-elastic light scattering is in good agreement with the average radius $\bar{r}$ derived from electron microscopy using the particle size distribution in Fig. 7 and Eqn. 5 (cf. Ref. 11):

$$\bar{r} = \frac{\Sigma n_i M_i^2 P_i(q)}{\Sigma n_i M_i^2 P_i(q) r_i^{-1}} \quad (5)$$

where n_i is the number of vesicles of radius r_i and

* The average radius $\bar{r}$ derived from Eqn. 5 is the z-average which is the same as that derived from quasi-elastic light scattering.

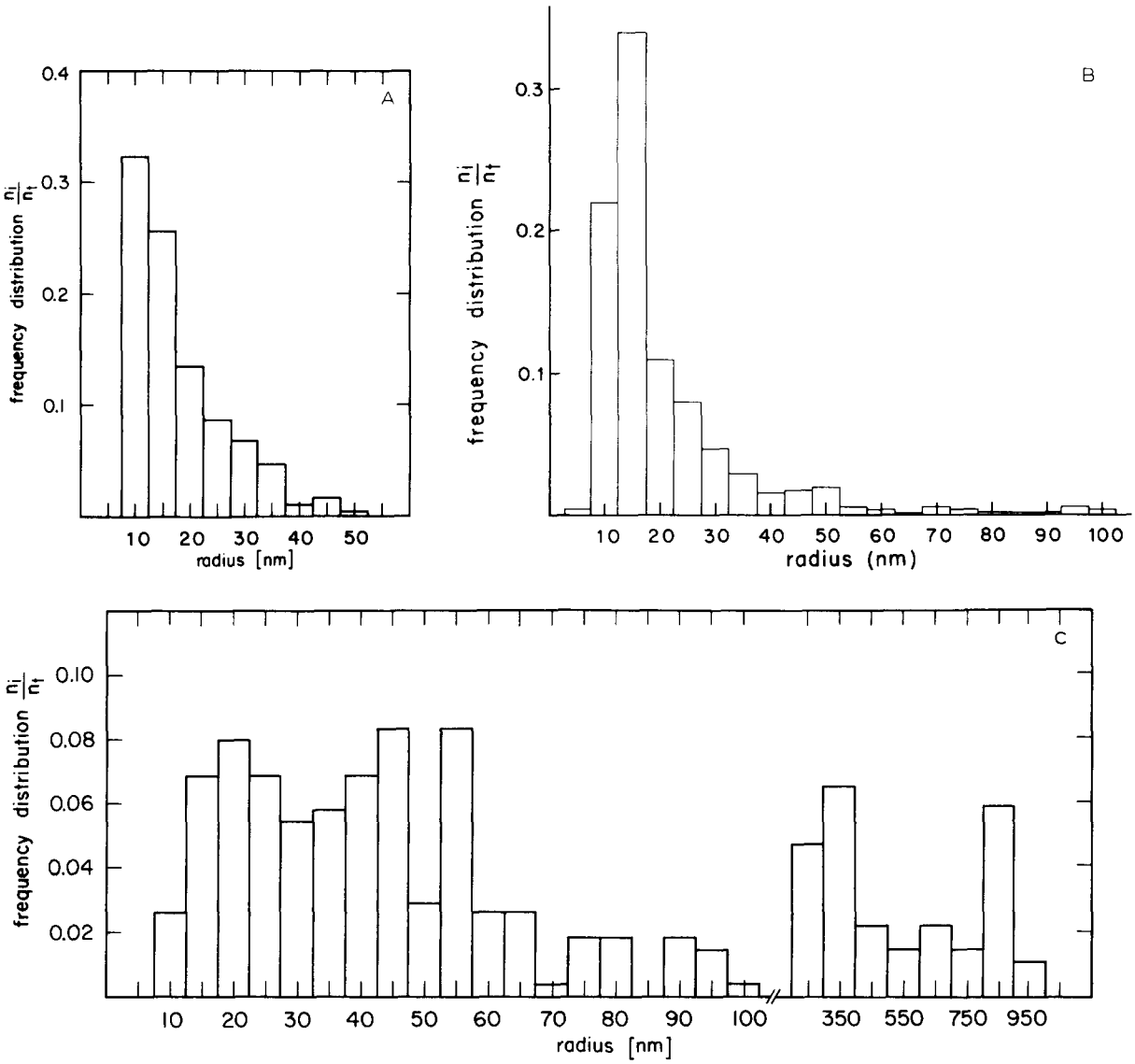

Fig. 7. A–C. Bar histograms derived from electron micrographs of freeze-fractured preparations of an unsonicated PA dispersion in water (A) and unsonicated mixed PA/PC dispersions in water, mole ratio, 1 : 1 (B) and mole ratio, 1 : 9 (C). 400–500 particles of each dispersion were measured. The relative frequency of a certain particle size of radius r_i is $n_i/\Sigma n_j$, where n_i is the number of particles with radius r_i. Vesicles with radii greater than the right-hand limit of the x-axis were still present in the dispersions shown in A and B, but since these vesicles made up a very small fraction and since the particle size distribution in that region was no longer continuous, they were not included in the diagram.

M_i is the vesicle weight which is proportional to $r_i^3 - (r_i - 5)^3$ (assuming a bilayer thickness of 5 nm). $P_i(q)$ is the scattering form factor calculated from the appropriate equation for a spherical shell [16]. For all dispersions investigated the polydispersity coefficient V calculated from a cumulant analysis of the intensity autocorrelation function was of the order of 50–100%, indicating a high degree of polydispersity. Based on this and the fact that the majority of samples gave two peaks on gel filtration (cf. Figs. 2, 3, and 5) we analyzed the intensity autocorrelation function in terms of a two-component distribution using Eqn. 3.

From the relative intensities G_i and the hydro-

dynamic radii r_i we also estimated the weight fractions W_i using Eqn. 6 (cf. Ref. 15):

$$W_i = \frac{G_i/M_iP_i(q)}{\Sigma G_i/M_iP_i(q)} \quad (6)$$

The values of r_i and W_i thus obtained are included in Table I. Inspection of this table shows that there is good agreement between the W_i values derived from the two-component analysis of the quasi-elastic light scattering data and the W_i values derived from gel filtratoin on Sepharose 4B. However, the Stokes radius of the small unilamellar vesicle population derived from gel filtration is significantly smaller than the corresponding r_2 values derived from the two-component fit of the quasi-elastic light scattering data. This discrepancy is most likely to be due to the fact that a rather heterogeneous phospholipid dispersion is analyzed in terms of an ideal two-component distribution. Freeze-fracture electron microscopy (Fig. 7) confirms the high degree of heterogeneity in the particle size distribution and reveals the presence of very large particles. Taking this into account a three component analysis of a 'spliced' correlation function (Eqn. 4) was considered to be more adequate. The results of such an analysis are summarized in Table II. The hydrodynamic radii r_3 thus obtained for the small unilamellar vesicle population are in reasonably good agreement with the Stokes radii derived from gel filtration (see Tables I–III).

As indicated in Figs. 2–6B, various fractions eluted from Sepharose 4B and Sephacryl S 1000 (Figs. 2–6A) were pooled and analyzed by quasi-elastic light scattering. Common to all dispersions shown in these figures, the mean hydrodynamic radius $\bar{r}_h$ decreased markedly with increasing fraction number (elution volume); however, the actual $\bar{r}_h$ values differed from dispersion to dispersion (Figs. 2–6B). Furthermore, $\bar{r}_h$ generally increased with increasing PC content. For reasons mentioned above, the intensity autocorrelation function obtained with various column fractions was analyzed in terms of a two-component distribution. The results of this analysis are also included in Figs. 2–6B. The two-component analysis of the PA dispersion shows that peak II consists predominantly ($W \simeq 97\%$) of small vesicles with a hydrodynamic radius of 11.0 ± 1.4 nm (Fig. 2B). With increasing PC content the weight fraction W_i of small vesicles decreased, whereas the hydrodynamic radius of this population increased (cf. Figs. 2–5B). The major component of the PA/PC dispersion (mole ratio, 1 : 1) eluted in peak II (Sepharose 4B) amounted to $W = 92$–95% and had a hydrodynamic radius of 17.5 ± 1 nm. The major component ($W = 93\%$) of the same PA/PC dispersion eluted in peak II from Sephacryl S 1000 (Fig. 5A) had a hydrodynamic radius of 20.0 ± 1.4 nm. In contrast, the vesicles in the trailing fractions of the peak obtained by gel filtration of the PA/PC dispersion (mole ratio, 1 : 9) (Fig. 4) represent the minor component ($W = 33.3\%$) with a hydrodynamic radius of 65 ± 8 nm. The dominant component in these fractions ($W = 66.7\%$) has a hydrodynamic radius of 230 nm.

The mean hydrodynamic radius $\bar{r}_h$ of vesicles eluted from Sepharose 4B in peak I was 75, 71 and 255 nm for pure PA, PA/PC (mole ratio, 1 : 1) and PA/PC dispersions (mole ratio, 1 : 9), respectively. The two-component analysis of vesicles eluted in peak I showed that with pure PA about 83% of the total phospholipid form vesicles with a hydrodynamic radius of 170 nm; in mixed PA/PC dispersions (mole ratio, 1 : 9) about 90% is present

TABLE II

THREE COMPONENT ANALYSIS OF QLS DATA RECORDED FROM UNFRACTIONATED PA AND PA/PC DISPERSIONS

Sample	r_1 (nm)	W_1 (%)	r_2 (nm)	W_2 (%)	r_3 (nm)	W_3 (%)
PA	181.8	40	56.2	13	14.0	47
PA/PC (mole ratio, 1 : 1)	400	7	58.5	32	17.5	61
PA/PC (mole ratio, 1 : 9)	403.1	55	106.1	28	26.1	17

TABLE III

COMPARISON OF THE PARTICLE SIZE ANALYSIS CARRIED OUT WITH THREE DIFFERENT METHODS

The radius of the small unilamellar vesicles present in unsonicated PA and mixed PA/PC (mole ratio, 1 : 1) dispersions in H_2O was determined by gel filtration, freeze-fracture electron microscopy and quasi-elastic light scattering (QLS). Explanation for quasi-elastic light scattering: (1) Fractionated: the lipid dispersion was chromatographed on Sepharose 4B and the fractions eluted in peak II were analyzed by quasi-elastic light scattering. The value in brackets was obtained after chromatographing the lipid dispersion on Sephacryl S 1000. (2) Unfractionated, the quasi-elastic light scattering results obtained with the original lipid dispersion were analyzed (cf. Table II) in terms of a three-component distribution using Eqn. 4.

Lipid dispersion	Gel filtration		Freeze-fracture electron microscopy	QLS	
	Sepharose 4B	Sephacryl S 1000		fractionated	unfractionated
PA	9.4	12	10	11	14
PA/PC	14.4	20	15	17.5(20)	17.5

as vesicles with a hydrodynamic radius of 263 nm. As shown for peak II, the hydrodynamic radius of both the minor and major component of peak I also increased with increasing PC content.

The quasi-elastic light scattering analysis of the PA/PC dispersions (mole ratio, 1 : 1) prepared in H_2O (Fig. 5B) should be compared with that of the same PA/PC dispersion prepared in the column buffer (Fig. 6B). For dispersions prepared in buffer instead of H_2O the mean hydrodynamic radius $\bar{r}_h$ and the radius of the dominant component of peak II were larger by a factor of about 2. This is consistent with the reduced elution volume of peak II observed in the Sephacryl S 1000 gel filtration pattern. The two-component analysis of peak II (Fig. 6B) showed that the weight fraction of small vesicles is reduced to about 82% (as compared to 93% in H_2O, cf. Fig. 5B) and that their hydrodynamic radius is increased to 45 ± 11 nm. In reasonable agreement, the Stokes radius of peak II derived from Sephacryl S 1000 gel filtration was 35 nm.

Electron microscopy

Electron micrographs of freeze-fractured preparations of pure PA and mixed PA/PC dispersions in H_2O were evaluated in terms of particle size distribution. Representative electron micrographs of such dispersions were published previously [3,5,6]. Both pure PA and mixed PA/PC dispersions consisted predominantly of small unilamellar vesicles (10 nm < vesicle radius < 50 nm, Fig. 7A and B). In additoin to small vesicles, large unilamellar vesicles were present the proportion of which appeared to increase with increasing PC content. This is entirely consistent with the gel filtration results. Multilamellar particles which are typical for unsonicated PC dispersions were scarce. However, the larger particles (radius greater than 200 nm) frequently contained smaller vesicles entrapped in their aqueous internal cavity. The particle size analysis of the three dispersions is shown in Fig. 7A–C. All three preparations are heterogeneous with non-Gaussian distributions. Consistent with the conclusions drawn from gel filtration and quasi-elastic light scattering, the smallest particles were observed with pure PA dispersions. The size of the dominant small vesicles derived from electron microscopy agrees well with both gel filtration and the quasi-elastic light scattering results (Table III). The radius of the small unilamellar vesicles present in PA and mixed PA/PC dispersions (mole ratio, 1 : 1) is 10 nm and 15 nm, respectively, as compared to 11 nm and 17.5 nm derived from quasi-elastic light scattering. It should be noted that the maximum in the PA dispersion at $r = 10$ nm may not represent the true maximum. This is probably due to the relatively large error of the measurement and the choice of presentation. In spite of the large error of the measurement it is clear from Fig. 7A–C that the maximum in the particle size distribution is shifted to larger values of r as the PC content increases.

Besides small unilamellar vesicles (r less than 50 nm), both the pure PA and the PA/PC (mole ratio, 1 : 1) dispersion contain large unilamellar vesicles (approx. 20% of the total vesicles) with a radius ranging between 50 and 400 nm (data not

shown). Compared to these two dispersions, the PA/PC dispersion (mole ratio, 1 : 9) is even more heterogeneous with several maxima between a vesicle radius of 20 and 450 nm (Fig. 7C). The proportion of large vesicles with a radius greater than 50 nm is significantly greater than in the other two dispersions, amounting to about 80% of the total vesicles measured.

Discussion

Unsonicated dispersions of pure PA and PA/PC mixtures were prepared by the method of transiently changing the pH as described previously [2–5]. The resulting dispersions are characterized in terms of particle size distribution using gel filtration, quasi-elastic light scattering and freeze-fracture electron microscopy. All three methods show that these dispersions are heterogeneous. PA dispersions consist mainly of small unilamellar vesicles (average radius 11 ± 2 nm). In PA/PC mixed dispersions the size of the small unilamellar vesicles increases with increasing PC content and at the same time the proportion of small unilamellar vesicles decreases. This is consistent with previous findings [5]. The smallest vesicles with a hydrodynamic radius of approx. 11 nm (Table III) are therefore obtained with pure negatively charged phosphatidic acid. That the size of the small unilamellar vesicles decreases with increasing quantities of charged PA is consistent with the model proposed by Israelachvili and his co-workers [19]. Consistent with this model is also the finding that the radius of the small unilamellar vesicles of the PA/PC dispersion (mole ratio, 1 : 1) is significantly increased if the dispersion is produced in the presence of salt rather than water. In the presence of salt the electrostatic repulsion between charged PA molecules is screened (cf. Figs. 5 and 6) and as a consequence the vesicle radius is increased.

A question of considerable interest is how the results derived from the three different methods compare quantitatively. Pertinent to this question is the information contained in Tables I and III. The agreement between the mean hydrodynamic radius $\bar{r}_h$ derived from a cumulant analysis of the quasi-elastic light scattering data and the corresponding average radius derived from freeze-fracture electron microscopy is satisfactory (cf. columns 1 and 2 of Table I). The objections that are frequently raised concerning a size distribution analysis by freeze-fracture electron microscopy are that such an analysis is tedious and that it might be subject to individual bias. Tedious it may be, but the good agreement between the electron microscopic data and the results obtained with two independent methods is encouraging and invalidates the latter objection. There is good agreement between the three different methods regarding the size determination of the small unilamellar vesicle population. This is evident from Table III. This table also indicates that there is good agreement between the gel filtration results obtained with two different column materials, Sepharose 4B and Sephacryl S 1000. The fact that the two columns were calibrated with chemically different compounds, i.e., with proteins and polystyrene particles, respectively, seems to be of little consequence, at least with the experimental error of our measurement. Sephacryl S 1000 has an exclusion diameter of about 300 nm which is significantly larger than that of Sepharose 4B (about 60 nm). As expected from this, the mean hydrodynamic radius (determined by quasi-elastic light scattering) of vesicles eluted from Sephacryl S 1000 in peak I is larger by a factor of about 2 compared to the corresponding Sepharose 4B peak. From the results presented here we can conclude that Sephacryl S 1000 lends itself well to the fractionation and size analysis of lipid vesicles. The advantages of Sephacryl S 1000 as a gel-exclusion medium have been discussed previously [9,17].

The average radius of the small unilamellar vesicles of PA and PA/PC (mole ratio, 1 : 1) derived from the three different methods used here (Table III) are 11 ± 2 and 17.5 ± 2 nm, respectively. These values are significantly smaller than those derived from the two-component analysis of the quasi-elastic light scattering data of an unfractionated lipid dispersion (cf. Table III). The discrepancy is probably due to the fact that quasi-elastic light scattering is very sensitive to even trace amounts of large vesicles. That this explanation is reasonable is also evident from the two-component analysis of fractions eluted under peak II (cf. Figs. 2 and 3). In these fractions the presence of very large particles can be ruled out and

indeed the hydrodynamic radius of the small unilamellar vesicle population derived by a two-component analysis of the quasi-elastic light scattering results is in close agreement with the average radius derived from gel filtration and electron microscopy (Table III). Therefore, in order to obtain meaningful results from quasi-elastic light scattering when applied to highly polydisperse samples it is useful to fractionate these samples according to size prior to the quasi-elastic light scattering measurement.

Gel filtration of Sepharose 4B does not give any information regarding the size of the particles eluted under peak I except that their size must exceed the exclusion diameter of this column material. So far, only a very approximate estimate of the size and size distribution of vesicles in peak I has been obtained from freeze-fracture electron microscopy [3,5,6]. Only the combination of gel filtration, quasi-elastic light scattering and electron microscopy as used in this work made a more detailed analysis of the large unilamellar vesicle population possible.

In conclusion, the spontaneous vesiculation induced in unsonicated PA and mixed PA/PC dispersions by a transient pH increase yields unilamellar vesicles which are rather heterogeneous with respect to size. This is particularly true for mixed PA/PC dispersions. With such heterogenous dispersions a detailed particle size analysis requires the combination of several physical techniques. As shown here, satisfactory results are obtained by fractionation of the heterogeneous vesicle dispersion on Sepharose 4B or Sephacryl S 1000 followed by the quasi-elastic light scattering analysis of the fractions thus obtained. One main conclusion which can be drawn from the work presented here is that the apparent mean radii determined by different techniques, e.g., gel filtration using calibrated columns of Sepharose 4B or Sephacryl S 1000, quasi-elastic light scattering and freeze-fracture electron microscopy are in good agreement with each other.

Acknowledgements

We thank Professor W. Känzig for his continuous support and his interest in this work. We wish to acknowledge the expert technical assistance of Mr. Jürg Baumann. We are indebted to Dr. Martin Müller and Dr. Ernst Wehrli for communicating the electron microscopy results. This work was supported by the Swiss National Science Foundation (Grant No. 3.156-1.81).

References

1 Szoka, F. and Papahadjopoulos, D. (1980) Annu. Rev. Biophys. Bioeng. 9, 467–508
2 Hauser, H. (1982) Trends Pharm. Sci. 3, 274–277
3 Hauser, H. and Gains, N. (1982) Proc. Natl. Acad. Sci. USA 79, 1683–1687
4 Gains, N. and Hauser, H. (1983) Biochim. Boiphys. Acta 731, 31–39
5 Hauser, H., Gains, N. and Müller, M. (1983) Biochemistry 22, 4775–4781
6 Hauser, H., Gains, N. and Lasic, D.D. (1984) in Physics of Amphiphiles, Micelles, Vesicles and Micro emulsions (Degiorgio, V. and Corti, M., eds.), North-Holland, Amsterdam
7 Brunner, J., Skrabal, P. and Hauser, H. (1976) Biochim. Biophys. Acta 455, 322–331
8 Ackers, G.K. (1967) J. Biol. Chem. 242, 3237–3238
9 Reynolds, J.A., Nozaki, Y. and Tanford, C. (1983) Anal. Biochem. 130, 471–474
10 Haller, H.R. (1980) Dissertation (6604) ETH Zürich
11 Schurtenberger, P., Mazer, N. and Känzig, W. (1983) J. Phys. Chem. 87, 308–315
12 Mazer, N.A., Benedek, G.B. and Carey, M.C. (1976) J. Phys. Chem. 80, 1075–1085
13 Koppel, D.E. (1972) J. Chem. Phys. 57, 4814–4820
14 Chu, B. (1974) Laser Light Scattering, Academic Press, New York
15 Mazer, N.A., Schurtenberger, P., Carey, M.C., Preisig, R., Weigand, K. and Känzig, W. (1984) Biochemistry 23, 1994–2005
16 Van de Hulst, H.C. (1957) Light Scattering by Small Particles, J. Wiley and Sons, London
17 Nozaki, Y., Lasic, D.D., Tanford, C. and Reynolds, J.A. (1982) Science 217, 366–367
18 Chen, P.S., Toribara, T.Y. and Warner, H. (1956) Anal. Chem. 28, 1756–1758
19 Israelachvili, J.N., Mitchell, D.J. and Ninham, B.W. (1977) Biochim. Biophys. Acta 470, 185–201